Remote Sensing Applications: Society and Environment 38 (2025) 101603

Contents lists available at ScienceDirect

Remote Sensing Applications: Society and Environment

journal homepage: www.elsevier.com/locate/rsase

Genetic Algorithm Optimized Multispectral Soil-Vegetation Drought Index (GA-MSVDI) for precision agriculture and drought monitoring in North Africa

Nasser A.M. Abdelrahim [a,b,c], Shuanggen Jin [a,d,*]

[a] Shanghai Astronomical Observatory, Chinese Academy of Sciences, Shanghai, 200030, China
[b] School of Astronomy and Space Science, University of Chinese Academy of Sciences, Beijing, 100049, China
[c] Civil Engineering Department, Faculty of Engineering, Sohag University, 82511, Egypt
[d] School of Surveying and Land Information Engineering, Henan Polytechnic University, Jiaozuo, 454003, China

ARTICLE INFO

Keywords:
Drought monitoring
High-resolution
Genetic algorithm
Soil moisture

ABSTRACT

Droughts are recurrent and persistent multi-hazard events that significantly impact ecosystems, agriculture, water supply, and economies. This study proposes the Genetic Algorithm-Optimized Multispectral Soil-Vegetation Drought Index (GA-MSVDI) for precision agriculture and drought assessment in Egypt's Nile Delta, El Kairouan in Tunisia, and Rabat-Salé-Kénitra in Morocco. This is based on the evaluation of soil moisture, vegetation health, and surface temperature from high-resolution satellite data derived from Landsat-8, Sentinel-1, and Sentinel-2. The Genetic Algorithm optimization process assigned the following weights: NDVI (0.24), NDII (0.20), LST (0.23), SMI (0.19), and SAVI (0.14). These weights underline, therefore, the requirement of Water content of vegetation and soil in drought detection, with NDVI and NDII being highly influential factors. The GA-MSVDI has been validated against existing indices like VHI for all seasons, which returned very high correlations ranging from 0.57 to 0.91 over the study areas. Compared to traditional indices such as NDVI, TCI, VCI, and SWCI, the proposed index demonstrated superior performance in capturing drought conditions across different climatic regions. This strong performance across various geographical regions and seasons proves GA-MSVDI to be a potential, reliable tool for accurate monitoring the drought in agricultural environments, particularly within water-scarce regions like North Africa.

1. Introduction

A significant natural calamity known as drought usually results from a lack of precipitation (Edokossi et al., 2024; Elameen et al., 2023; Jin and Zhang, 2016; West et al., 2019). Droughts can be classified as meteorological, agricultural, hydrological, or socioeconomic by the American Meteorological Association (Esfahanian et al., 2016; Li et al., 2024). A very low precipitation spell lasting several months or even years is known as a meteorological drought; Groundwater, streamflow, or total water storage that is lower than long-term averages result in a hydrological drought; Dry conditions that result in higher demand than supply for specific goods are referred to as socioeconomic droughts. When soil moisture levels fall below what is necessary for plants to function properly, agricultural drought breaks out (Alahacoon et al., 2021; Hao et al., 2015; Jiao et al., 2019; Yao et al., 2020). A crop's output can be

* Corresponding author. Shanghai Astronomical Observatory, Chinese Academy of Sciences, Shanghai, 200030, China.
E-mail addresses: sgjin@shao.ac.cn, sg.jin@yahoo.com (S. Jin).

https://doi.org/10.1016/j.rsase.2025.101603
Received 27 August 2024; Received in revised form 26 March 2025; Accepted 19 May 2025
Available online 20 May 2025

significantly decreased by an agricultural drought, which is often a brief period of dryness (a few weeks), but it happens at a crucial point in the growth season (Heim, 2002; Zhang et al., 2013).

Establishing a nationwide drought strategy or policy requires the creation of an extensive mechanism for monitoring droughts that can promptly give a heads-up of a drought's beginning, the degree, time, and area of coverage (Hayes et al., 2011). The factors that are utilized to describe the physical features of drought, such as its length, intensity, and spatial extent, are known as drought indicators and indices. Indices are usually computationally generated numerical severity descriptions or extent of a drought; on the other hand, indicators are broader terms that encompass characteristics like temperature, streamflow, rainfall, and drought indices (Hao and Singh, 2015; Hayes et al., 2012). Many drought indices have been developed in order to track and measure drought. To measure drought, each drought indices needs a set of input parameters (Dai, 2011; Esfahanian et al., 2017). Depending on drought type, drought indices were categorized and then separated into conventional/region-specific and remote sensing categories based on the type of data used. Additionally, simple indices including microwave, thermal, and optical as well as composite indices were separated out of the drought indices based on type remote sensing (Alahacoon and Edirisinghe, 2022; Holben, 1980; Felegari et al., 2021). Palmer Drought Severity Index (PDSI) (Li and Cai, 2024; Palmer, 1965), Standardized Precipitation Index (SPI) (Sakellariou et al., 2024), and Standardized Precipitation Evapotranspiration Index (SPEI) (Dong et al., 2023; Vicente-Serrano et al., 2010) are the most commonly used drought indices derived from site data. These indices, which primarily offer precise assessments of agricultural drought conditions in specific places, depend on agroclimatic stations' in-situ readings of soil moisture, evapotranspiration, and precipitation. Nevertheless, because of their sparse distribution and small number, these agroclimatic stations lack the geographical representative aspect of agricultural drought (Hazaymeh and Hassan, 2017).

Assessment of the drought has benefited greatly over the past few years by the use of high-resolution model data and remote sensing (Abdelrahim and Jin, 2025; Edokossi et al., 2020; Jin et al., 2022, 2024; Najibi and Jin, 2013). Given its broad geographic coverage and reasonably good temporal and spatial precision, satellite imagery is a useful tool for monitoring drought. When there are few sample gauges in a given area, remote sensing data could be the only source of information accessible for tracking drought (Farrag et al., 2020; Gaber et al., 2021; Jiao et al., 2016; Wu, 2013). Currently, most studies were concentrated on the creation of concepts for drought monitoring and indices using data from remote sensing for various applications (Afshar et al., 2021; Araneda-Cabrera et al., 2021; Corbari et al., 2024; Dos Santos Araujo et al., 2024; Li et al., 2024; Qin et al., 2021; Sánchez et al., 2016; Schwabe et al., 2013; Shahzaman et al., 2021; Skakun et al., 2016; Tang and Li, 2014; Tian et al., 2018; Zhang et al., 2017), such as the normalized difference vegetation index (NDVI) (Thenkabail et al., 1994), Shortwave Infrared Water Stress Index (SIWSI) (Fensholt and Sandholt, 2003), Visible and Shortwave Drought Index (VSDI) (Zhang et al., 2013), Vegetation Condition Index (VCI) (F.N. Kogan, 1995), Soil Adjusted Vegetation Index (SAVI) (Huete, 1988), Temperature Condition Index (TCI) (Kogan, 1997), Normalized Difference Infrared Indexes (NDII) (Fensholt and Sandholt, 2003), Vegetation Health Index (VHI) (Alahacoon et al., 2021; Bhuiyan et al., 2006), and Soil Moisture Condition Index (SMCI) (Zhang and Jia, 2013).

High-resolution data on the state of agricultural drought that is continuously captured, both geographically and temporally, is needed to address this increased risk of drought (Dotzler et al., 2015). More and more, near-real-time, multi-temporal, and regional Earth observation (EO) applications using Sentinel-2 (S2) sceneries are being used (Sudmanns et al., 2020). The restricted availability of optical data resulting from cloud cover is a significant drawback. However, because of their ability to gather data concerning any weather circumstances and at night, Synthetic Aperture Radar (SAR) systems like Sentinel-1 (S1) may be able to significantly close these monitoring gaps (Felegari et al., 2021; Kaiser et al., 2022). Understanding the earth's surface's thermal behavior and drought monitoring depend heavily on LST estimation, or land surface temperature estimation (Pande et al., 2024). Using Google Earth Engine GEE (Mullissa et al., 2021; Teluguntla et al., 2018), a cloud-based platform that makes remote sensing data analysis and processing easier, is one of the efficient ways to estimate LST. Thermal infrared data from sensors such as Landsat-8 is among the several satellite imagery options provided by GEE (Pande et al., 2023; Ren et al., 2021). Using time series that illustrate surface processes, the increased availability of data opens up new possibilities for temporal as well as spatial data analysis (Urban et al., 2018).

The majority of current drought indices rely on coarse resolution data with a range of 250 m to 1 km, despite notable improvements in drought monitoring. The localized subtleties of drought conditions are frequently missed by these intermediate to coarse resolution datasets, such those from MODIS, especially in varied environments. Additionally, very little research has been done on drought monitoring in Africa, a continent that is extremely susceptible to both water scarcity and climate variability (Atzberger, 2013; Brandt et al., 2016; Malakar and Hulley, 2016; Tran et al., 2017; Trnka et al., 2020; Winkler et al., 2017). However, the fact that these integrated, remotely-sensed indices were created and assessed for a particular climatic or geographic area severely limits their applicability (Zhang et al., 2017). Generally, the indices were established across study areas that are limited to a single climate region. A small number of these indices were created in a variety of settings spanning wide geographic areas. If specific indices are utilized in climate zones that differ significantly from those in which they were established, this geographic restriction may result in subpar performance (Quiring and Ganesh, 2010).

This research aims to address these gaps by developing Genetic Algorithm Optimized Multispectral Soil-Vegetation Drought Index (GA-MSVDI) using high-resolution (10 m) Landsat, Sentinel-2, and Sentinel-1 data by integrating multiple indices through genetic algorithms. Unlike prevailing pre-defined weighted drought indices or those using mono-sensor inputs, GA-MSVDI utilizes an optimization technique to distribute adaptive weights over remote sensing indexes for flexibility to diverse climatic regimes. Using Google Earth Engine GEE and Python all calculations were carried out. This approach not only enhances spatial resolution but also offers timely and accurate drought information, which is essential to efficient resource administration and policy-making in drought-prone regions of North Africa. The rest of this paper is consistent of materials and methods in Section 2, Section 3 contains results, analysis and discussions, and the conclusion is given at Section 4.

2. Materials and methods

2.1. Study areas

The study area covers approximately 68,000 km2 distributed in it. The three parts of North Africa include the Nile Delta portion in Egypt, El Kairouan and surrounding in Tunisia, and Rabat-Salé-Kénitra in Morocco. The most important agricultural place in Egypt is the Nile Delta. It stands between latitudes 30°00′ N and 31°30′ N, and longitudes 31°00′ E and 32°30′ E. Fertile soils and a flat topography make the Delta one of the agricultural zones with the highest productivity of the country (Moursy et al., 2023). Annual Rainfall - Less than 200 mm on an average per year. Rainfall Variation - Practically nil, since less than 200 mm of rainfall occurs annually on Egypt's Mediterranean coast. Rainfall decreases from the north towards the south in the Nile Delta. Cropping Season are two crops in the country. They are the main cropping period, from April to September, which is the season of maximum need of water, and the winter cropping, from October to March. Cereals like sugar cane, rice, cotton, and maize are cultivated during the summertime, while wheat, clover, and beans are grown in winter (Ayyad et al., 2019; Ewis Omran and Negm, 2020).

El Kairouan and its environs are famous for olive production, and it is one of the hottest prefectures in Tunisia. Geographically, it lies between approximately 36°10′N and 35°10′N latitude and 09°35′E and 10°20′E longitude (Al Saud, 2022). The semi-arid climate has varying characteristics according to seasonal changes. In the wet season, which runs from October until March, the amount of rainfall highly changes between 200 and 500 mm, or less (Salem et al., 2023; Zekri, 2020).

Rabat-Salé-Kénitra is located in the northwest of the state of Morocco, generally between latitudes 35°00′N and 33°90′N, and between longitudes 06°40′W and 05°20′W (Amiri et al., 2021), with roughly 600 mm of annual rainfall on average. It has a Mediterranean climate, which means it features hot summers, mainly dry, and warm winters with a rainy period running from November to March (Behnassi et al., 2021; Schilling et al., 2020). The three study areas are illustrated in Fig. 1, and summarized in Table 1.

2.2. Data acquisition

To ensure comprehensive coverage of the study areas, we utilized high-resolution satellite images with minimal cloud coverage (less than 10 %) from the Landsat-8, Sentinel-2 (S2), and Sentinel-1 (S1) satellites. These images were sourced using Google Earth Engine (GEE), a robust cloud-computing platform that facilitates large-scale environmental data analysis. The selected timeframe for data collection spanned to three months from January to March, from April to June, from Juley to September, and from October to December. The data collection period included the year 2020, the study could be performed on any year staring from 2015, when the satellite S1 had been lunched. Table 2 summarized data information.

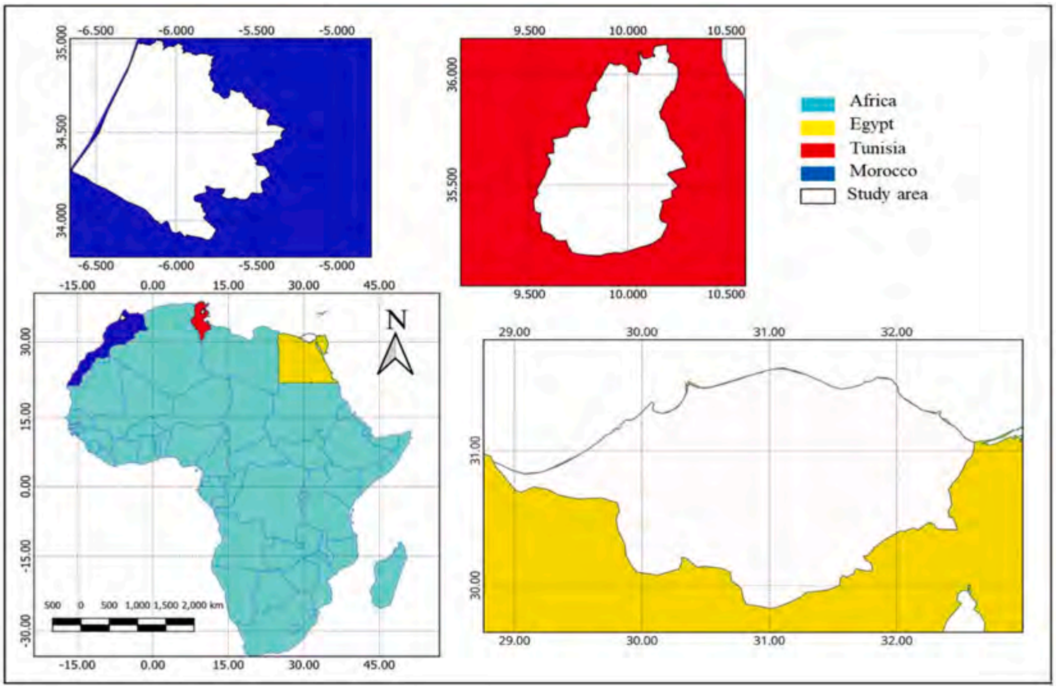

Fig. 1. Geographical representation of the study areas, including the Nile Delta (Egypt), El Kairouan (Tunisia), and Rabat-Salé-Kénitra (Morocco).

Table 1
A summary of key attributes for the three study areas, including climate classification, average annual rainfall, cropping seasons, and dominant crops cultivated in each region.

Location	Climate	Main Crops	Rainfall (mm/year)	Rainfall Season	Area (km^2)
Nile Delta, Egypt	Mediterranean, very limited rainfall	Summer: sugar cane, rice, cotton, maize Winter: Wheat, clover, beans	~200 (only on Mediterranean coast)	October to March	55,698
El Kairouan, Tunisia	Semi-arid, high seasonal variation	Olives, barley, wheat, pomegranates, figs, tomatoes, peppers, chickpeas, lentils, alfalfa	200–500	October to March	4779
Rabat-Salé-Kénitra, Morocco	Mediterranean, hot dry summers, mild wet winters	wheat, barley, potatoes, tomatoes, carrots, citrus, grapes, apples, olives, beans, peas, alfalfa	~600	November to March	8338

Table 2
Summary of satellite datasets, including source, spatial resolution, and revisit frequency.

Data Type	Dataset Name	Source	Spatial Resolution	Temporal Resolution
Sentinel-1 (S1)	COPERNICUS/S1_GRD	ESA	10 m	6 days
Sentinel-2 (S2)	COPERNICUS/S2_SR	ESA	10 m	5 days
Landsat-8	LANDSAT/LC08/C02/T1_L2	USGS	30 m	16 days

2.3. Methodology

Below is the flowchart used in developing the methodology of the Genetic Algorithm Optimized Multispectral Soil-Vegetation Drought Index as shown in Fig. 2. Data gathering from the three important satellite sources, S1, S2, and Landsat-8, constitutes the very first step of the process in this study. The S1 radar data are considered to represent the soil moisture after a series of preprocessing, such as noise reduction and terrain correction. This way, we can make sure that the data is correct and ready to be analyzed. Meanwhile, S2 and Landsat-8 provide optical data to be used in computing several vegetation indices, such as NDVI, NDII, SAVI, and LST. These indices help us understand the health of vegetation, soil moisture levels, and temperature at the surface, all of which are essential indicators of drought.

Once prepared, your data is fed into a system based on Genetic Algorithms. In the first place, this system normalizes the data to ensure that all the inputs are comparable. Then, the GA is fine-tuned to identify the best combination of these indices to accurately reflect drought conditions. The GA process is iterative: it begins by generating a range of potential solutions, evaluates how well each one performs, and then refines the best solutions through selection, crossover, and mutation techniques. This process continues until the most effective solution is found.

Finally, the optimized outputs from the GA are used to generate the GA-MSVDI, which is subsequently used to produce drought

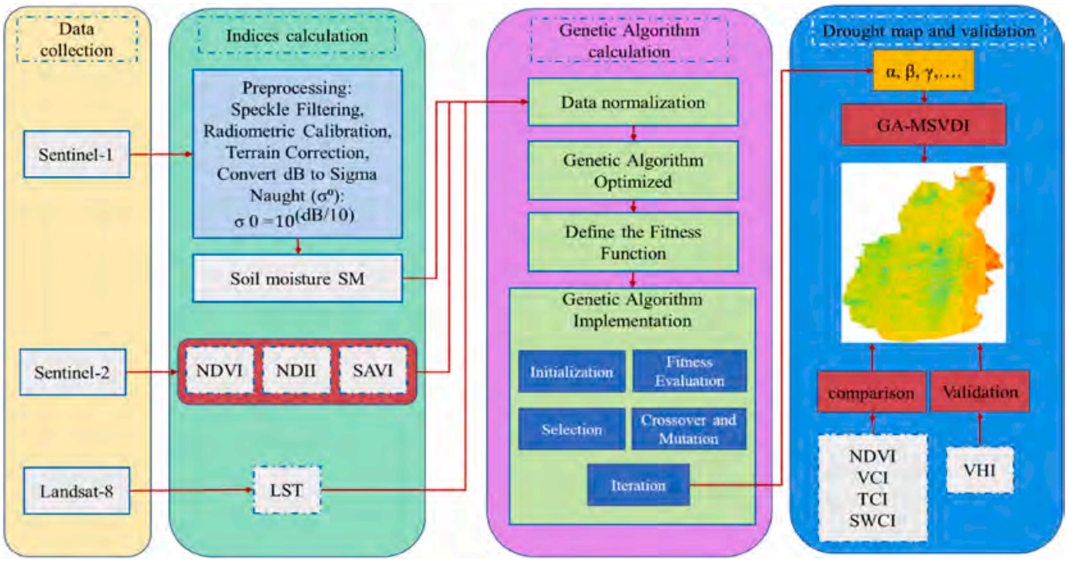

Fig. 2. A detailed flowchart illustrating the step-by-step methodology used to develop the Genetic Algorithm-Optimized Multispectral Soil-Vegetation Drought Index (GA-MSVDI). The process includes data acquisition, preprocessing, feature selection, Genetic Algorithm (GA) optimization, drought index computation, and validation against established drought indices.

maps. These maps are validated and compared against existing indices like NDVI (Normalized difference vegetation index), VCI (Vegetation Condition Index), TCI (Temperature Condition Index), and SWCI (Soil Water Content Index), as well as the Vegetation Health Index (VHI), to ensure the reliability and accuracy of the new index. This comprehensive methodology leverages multi-source data and advanced optimization techniques to develop a high-resolution drought monitoring tool tailored for agricultural applications in North Africa. This thorough testing across multiple areas underscores the index's robustness and suitability for broad application, particularly in regions like North Africa where accurate drought monitoring is critical.

2.3.1. Remote sensing indices

2.3.1.1. Normalized Difference Vegetation Index NDVI. The NDVI, whose index values change according to variations in vegetation conditions, can be used as a guide for areas with irrigation since it shows the amount of green biomass (Brown and Pervez, 2014; Pervez and Brown, 2010). The NDVI is highly impacted by the weather, with arid and semi-arid regions being more affected than other places (Sardooi et al., 2021). NDVI time series data with a temporal resolution of 5 days and a geographical resolution of 10 m can potentially be obtained by high spatial satellites like Sentinel-2. For the purpose of drought monitoring, it can be utilized to identify distinct multi-temporal, spectral vegetation patterns (Chen et al., 2023). NDVI was calculated using the famous formula in eq. (1) (Afshar et al., 2021).

$$\mathrm{NDVI} = \frac{(\mathrm{NIR} - \mathrm{RED})}{(\mathrm{NIR} + \mathrm{RED})} \tag{1}$$

where NIR is the near infra-red band and RED is the red band.

2.3.1.2. Soil Adjusted Vegetation Index SAVI. Spectral signatures of different forms of land cover are not the same as those of soil. Reflectance rises in direct proportion to wavelength increases in the visible and near-infrared regions. Nonetheless, a number of factors influence the rate of increase. The reflectance of soil can be reduced by both soil moisture and organic materials. For a variety of soil types and physiognomies, the relationship between near-infrared and red reflectance is consistent. The two values are connected and exhibit a linear connection with changes in the moisture content (Binte Mostafiz et al., 2021; Konno and Homma, 2023; Rhyma et al., 2020). For every kind of soil, there is a very unique relationship. To take into consideration the impact of soil brightness in areas with a restricted amount of vegetation, the L coefficient (which is assumed in this work to be equal to 0.5) is added to the computation of SAVI, which is determined using formula eq. (3) from NIR and RED (Huete, 1988; González-Gómez et al., 2022).

$$\mathrm{SAVI} = \frac{(\mathrm{NIR} - \mathrm{RED})}{(\mathrm{NIR} + \mathrm{RED} + \mathrm{L})} * (1 + \mathrm{L}) \tag{3}$$

2.3.1.3. Normalized Difference Infrared Index NDII. Using ratios of various near infrared reflectance (NIR) and shortwave infrared reflectance (SWIR) values as defined by eq. (4), the NDII was created (Fensholt and Sandholt, 2003; Mathivha and Mbatha, 2021).

$$\mathrm{NDII} = \frac{(\mathrm{NIR} - \mathrm{SWIR1})}{(\mathrm{NIR} + \mathrm{SWIR1})} \tag{4}$$

Owing to the leaf's high absorption, the NDII's shortwave infrared reflectance property, which is negatively correlated with leaf water content and offers further details on the water that is available for vegetation to use in the soil, can be used to both detect plant water stress and measure vegetation's water content (Mbatha and Xulu, 2018; Sriwongsitanon et al., 2016).

2.3.1.4. Land Surface Temperature LST. The temperature of the topmost layer of soil LST has a major effect on the output of agricultural crops, the need for water, and the rise in area mortality that occurs throughout the summer. It has long been known that plant temperature serves as a reliable predictor of water availability. The irrigation-induced change in the LST gap between day and night was reflected using temperature data collected both during the day and at night (Abdulmana et al., 2021; Arabi Aliabad et al., 2023). To compute LST, Thermal Infrared Sensor (TIRS) and Landsat Operational Land Imager (OLI) time series of Landsat images large-scale environmental data analysis was produced using GEE (Begum et al., 2021; Pande et al., 2024).

2.3.1.5. Soil Moisture Index SMI. Weather forecasting and drought monitoring both require an understanding of soil moisture content (Mishra et al., 2017). Due to the fact that aperture radar (SAR) sensors can detect the target's geometrical and dielectric properties, they provide an effective means of mapping and tracking soil moisture. Furthermore, Weather does not affect SAR acquisitions, which gives them a major edge over optical imaging when there is cloud cover. Vegetation cover, however, complicates these processes and affects how the combined effects of soil moisture and vegetation cover interact with SAR backscatter (Bhogapurapu et al., 2022a, 2022b; Chaudhary et al., 2022). In order to do this, average surface soil moisture values are calculated using equation (5). An indicator of soil moisture that has a value ranging from 0 to 1, where 0 denotes the most dry soil conditions and 1 denotes the most wet soil conditions (Foucras et al., 2020)

$$\mathrm{SMI} = \frac{(\sigma\mathrm{VV} - \sigma\mathrm{VVmin})}{(\sigma\mathrm{VVmax} - \sigma\mathrm{VVmin})} \tag{5}$$

VV (Vertical transmit, Vertical receive), σVV is the backscatter at a given time, σVVmin and σVVmax are the minimum and maximum backscatter values observed over the time series, representing very dry and very wet conditions, respectively.

2.3.2. Genetic Algorithm (GA) Optimization

Genetic algorithm is the most popular optimization methods (Chen et al., 2022). The objective is to determine the ideal weights for each index (SMI, NDVI, NDII, LST, SAVI) to maximize the correlation with drought measurements (Kaur and Sood, 2020). Fig. 3 illustrate the concept and steps of GA.

a) Initialization

Start by creating an initial population of potential solutions. Each solution is a unique set of weights assigned to the drought indices (SMI, NDVI, NDII, LST, SAVI). Each index's contribution to the final GA-MSVDI is determined by these weights (Dey, 2023; Gad, 2023; Katoch et al., 2021).

b) Fitness Evaluation

Assess each solution by calculating a fitness score. The score would be based on the weighted average of the indices such that the correlation against drought measurements such as the VHI or VDI is maximized and the better the correlation, the higher the fitness score (Dey, 2023; Gad, 2023; Razavi-Termeh et al., 2023).

c) Selection, Crossover, and Mutation

Assess each population member's fitness score to determine which of their solutions performs best. These top solutions are more likely to produce better offspring in the next generation. Pair the selected solutions and perform crossover operations. In this step, portions of the weights from two parent solutions are exchanged to create new offspring. This helps combine favorable characteristics from different solutions. Introduce small, random changes (mutations) to some of the offspring's weights. This step is crucial for maintaining diversity within the population and for exploring new areas of the solution space that may lead to better results (Dey, 2023; Gad, 2023; Katoch et al., 2021; Razavi-Termeh et al., 2023).

d) Iteration

Repeat the process of fitness evaluation, selection, crossover, and mutation over multiple generations. With each generation, the algorithm refines the solutions, gradually improving the weight combinations. Continue iterating until the algorithm converges, meaning that further generations do not produce significantly better solutions. At this point, the best set of weights has been identified (Dey, 2023; Katoch et al., 2021; Razavi-Termeh et al., 2023).

e) Final Output

The algorithm outputs the optimized set of weights for the GA-MSVDI. These weights are then used to combine the indices as illustrated in eq. (6)., resulting in a highly accurate drought index that correlates well with actual drought conditions (Dey, 2023; Gad, 2023; Katoch et al., 2021; Razavi-Termeh et al., 2023).

$$\text{GA-MSVDI} = w_1 * \text{NDVI} + w_2 * \text{SMI} + w_3 * \text{NDII} + w_4 * \text{SAVI} + w_5 * \text{LST} \tag{6}$$

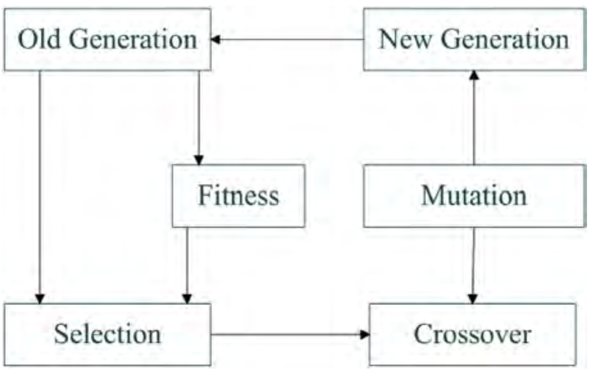

Fig. 3. Illustration of the Genetic Algorithm's optimization process, demonstrating how multiple drought-related parameters are weighted and integrated into GA-MSVDI for improved drought assessment.

2.3.3. Validation and performance assessment of GA-MSVDI

Validation is a crucial stage in the creation of a drought index, as it evaluates the index's accuracy in characterizing droughts (Bhuyan-Erhardt et al., 2019; Hao and AghaKouchak, 2014). Comparing a drought index's temporal and spatial data with other widely recognized drought indices is a frequently used method of validation (Hao and Singh, 2015; Zhou et al., 2013).

GA-MSVDI is validated against established drought indices such as the Vegetation Health Index (VHI). The VHI is one of the most commonly used remote sensing drought indicators (Bento et al., 2018; Pei et al., 2018; Shahzaman et al., 2021). Its definition is the simple average of two elements, VCI and TCI, which are obtained from data on the visual and thermal bands, respectively. (Bento et al., 2020; Qin et al., 2021).

To determine whether GA-MSVDI is suitable for drought monitoring, a performance evaluation of the system is required (Bayissa et al., 2018; Wable et al., 2019). The study evaluated the performance of five drought indices (GA-MSVDI, NDVI (Afshar et al., 2021), SWCI (Chen et al., 2020), TCI and VCI (Bento et al., 2020; Qin et al., 2021). The correlation between VHI and the other five drought indices was calculated to evaluate the performance of each other.

3. Results and discussions

3.1. GA-MSVDI equation

Weights returned by the Genetic Algorithm Optimization process for the indices were as follows: SMI is 0.19, NDVI is 0.24, NDII is 0.20, SAVI is 0.14, LST is 0.23. The combined weights of SMI and NDII are 0.39, simply indicating that these two indices representing soil moisture and vegetation water content are the two most contributing factors to the drought index. This goes to underline the critical role of soil and vegetation water status in detecting drought conditions, particularly in agricultural monitoring. The next most influencing factor is NDVI, relating to general health and greenness of vegetation with a weight of 0.24. LST, at 0.23, also plays an important role, underscoring the importance of temperature in assessing drought severity. The relatively lower weight of SAVI (0.14) suggests its specific but less dominant role in the overall index. This weighting scheme effectively prioritizes the most critical factors for accurate drought monitoring, particularly in regions with varying soil moisture and vegetation conditions.

3.2. Validation

To assess GA-MSVDI accuracy, the correlation between VHI and GA-MSVDI was calculated. Figures (4-6) show the correlation coefficient between GA-MSVDI and VHI in the three study areas and Table 3 summarize these correlation coefficients. The correlation

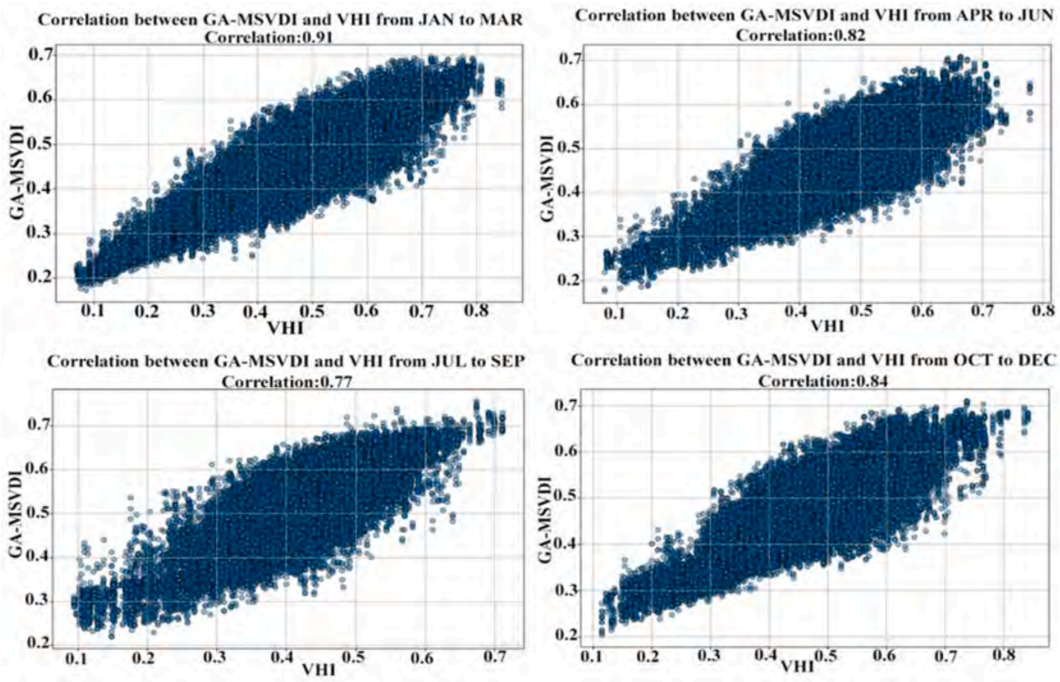

Fig. 4. Scatter plot showing the correlation between GA-MSVDI and VHI in the Nile Delta. The Pearson correlation coefficient (r) ranges from 0.77 to 0.91, indicating a strong agreement and confirming GA-MSVDI's reliability in detecting drought conditions.

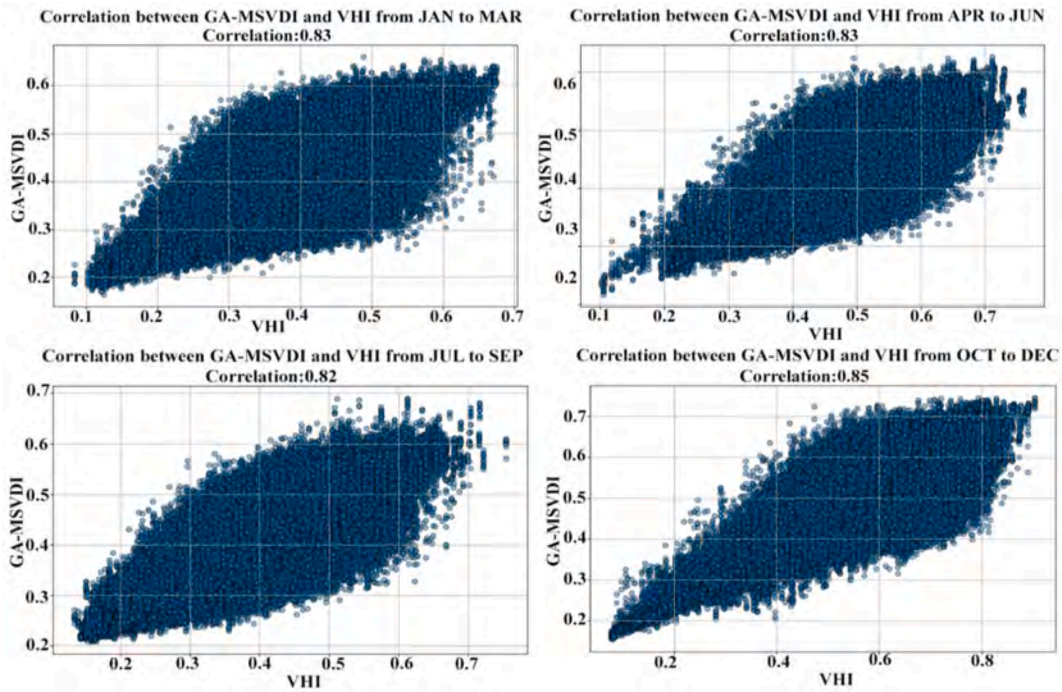

Fig. 5. Scatter plot of GA-MSVDI vs. VHI in El Kairouan. The Pearson correlation coefficient (r) ranges from 0.82 to 0.85, demonstrating the index's strong performance in semi-arid agricultural regions.

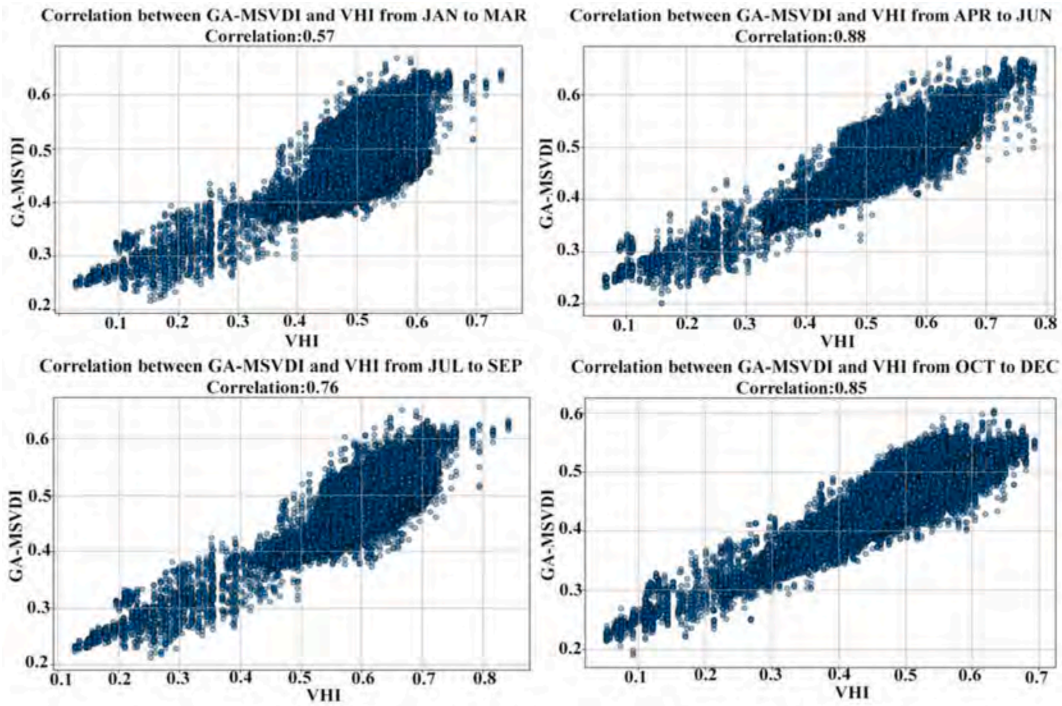

Fig. 6. Scatter plot of GA-MSVDI vs. VHI in Rabat-Salé-Kénitra. The Pearson correlation coefficient (r) ranges from 0.57 to 0.88, confirming GA-MSVDI's effectiveness in capturing drought variability in a complex climate.

Table 3
A quantitative comparison of GA-MSVDI's correlation (Pearson correlation) with VHI for each study area across four seasons. The results confirm that GA-MSVDI consistently maintains higher correlation values (0.57–0.91) compared to traditional indices, validating its effectiveness in monitoring drought conditions.

Date / Study area	JAN-MAR	APR-JUN	JUL-SEP	OCT-DEC
Nile delta	0.91	0.82	0.74	0.84
El Kairouan	0.83	0.83	0.82	0.85
Rabat-Salé-Kénitra	0.57	0.88	0.76	0.85

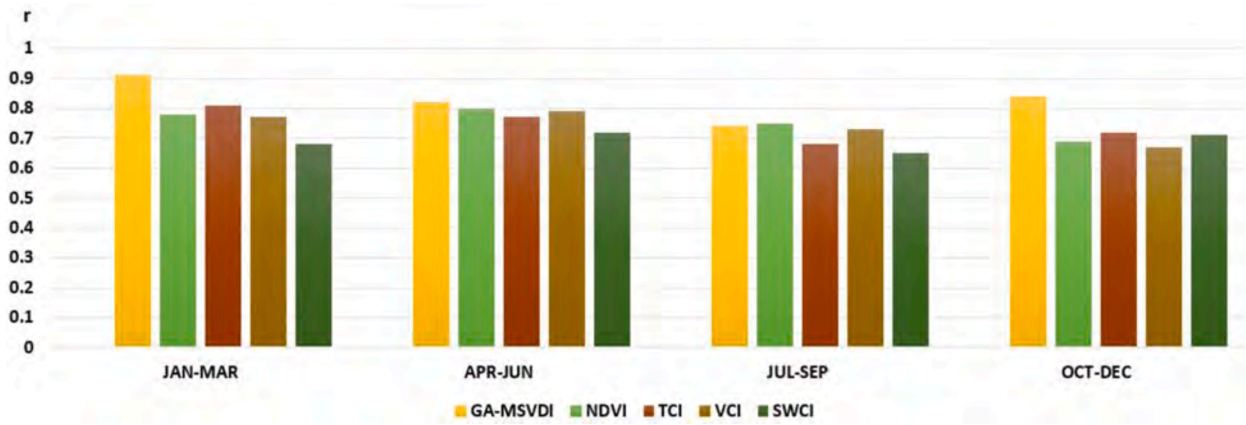

Fig. 7. Comparison of GA-MSVDI with NDVI, TCI, VCI, and SWCI in the Nile Delta across four seasons. GA-MSVDI shows the highest Pearson correlation with VHI (0.77–0.91), outperforming NDVI (0.69–0.80), TCI (0.68–0.81), VCI (0.67–0.79), and SWCI (0.65–0.72), confirming its superior accuracy in detecting drought conditions.

Fig. 8. Seasonal comparison of GA-MSVDI with NDVI, TCI, VCI, and SWCI in El Kairouan. GA-MSVDI maintains the highest correlation with VHI (0.82–0.85), surpassing NDVI (0.71–0.81), TCI (0.69–0.79), VCI (0.70–0.79), and SWCI (0.68–0.75), highlighting its effectiveness in semi-arid agricultural regions.

between VHI and the other drought indices was calculated to assess how well the drought indexes performed. Figures (7-9) illustrate the correlation values between VHI and GA-MSVDI, NDVI, SWCI, VCI and TCI.

3.3. *Drought maps*

The drought maps as shown at figures 10–12 generated using the newly developed high-resolution drought index GA-MSVDI provide a detailed spatial representation of drought severity across the study areas. These maps further integrate the optimized weights from the Genetic Algorithm and thereby represent the combined effects of SMI, NDVI, NDII, SAVI, and LST. Based on this integrated assessment of the condition of soil water content and vegetation health, the visual outputs highlight the areas that are

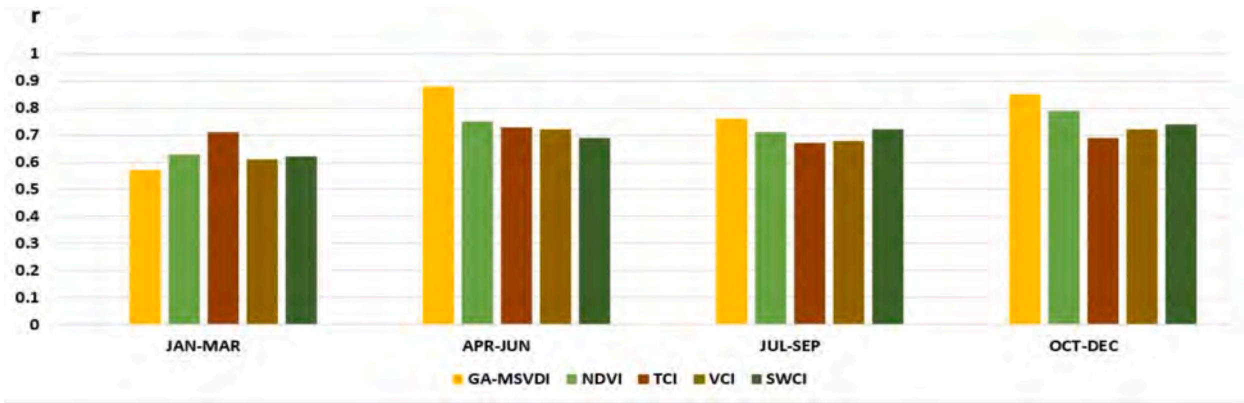

Fig. 9. Performance comparison of GA-MSVDI with NDVI, TCI, VCI, and SWCI in Rabat-Salé-Kénitra. GA-MSVDI achieves the highest correlation with VHI (0.57–0.88), outperforming NDVI (0.63–0.79), TCI (0.67–0.73), VCI (0.61–0.72), and SWCI (0.62–0.74), demonstrating its reliability in capturing drought variability in a complex climate.

suffering from mild to severe drought conditions.

The maps also reveal the temporal dynamics of drought, showcasing how drought conditions evolve and spread over time. These visual tools are essential for stakeholders, providing actionable insights for drought preparedness and management, especially in agriculture-dependent regions where timely intervention can mitigate the impact on crop yields and water resources. The resulting drought maps closely align with the precipitation and temperature patterns observed on the Climate Maps website as shown at figures 13 and 14, accessed on August 24, 2024, at climatemaps.romgens.com. This correlation underscores the reliability of the recently created drought index in identifying real-time drought conditions. Areas identified as drought-prone in the drought maps correspond well with regions experiencing lower precipitation and higher temperatures, as indicated by the climate data. This consistency across datasets reinforces the validity of the drought maps as a powerful tool for assessing drought severity and making informed decisions for resource management and agricultural planning.

3.4. Analysis

The results for the GA-MSVDI reveals that this newly developed index demonstrates strong and consistent performance across all three study areas. Over the whole year, GA-MSVDI has a very high correlation coefficient from 0.74 to 0.91 with VHI in the Nile Delta. This indicates that the index is highly effective for capturing drought conditions in this very important agricultural region wherein accurate monitoring is of decisive significance for water resource and crop production management. The comparison with other established indices, such as NDVI, TCI, VCI, and SWCI, further highlights the superior performance of GA-MSVDI, especially in the April–June period, where it outperforms NDVI, TCI, VCI, and SWCI, demonstrating its robustness.

In El Kairouan, Tunisia, GA-MSVDI also shows high correlation values, consistently above 0.80, indicating its reliability in a semi-arid climate with high seasonal variability. The comparison shows that while NDVI performs relatively well, GA-MSVDI provides a more comprehensive assessment, particularly during the summer months when drought conditions are more pronounced. Rabat-Salé-Kénitra in Morocco presents a slightly more variable performance, with GA-MSVDI correlation coefficients ranging from 0.57 to 0.88. However, during the critical April–June and October–December periods, GA-MSVDI exhibits strong correlations (0.88 and 0.85, respectively), surpassing other indices. This suggests that GA-MSVDI is particularly effective during key agricultural seasons, aligning well with observed precipitation and temperature patterns.

The results validate GA-MSVDI as a highly reliable and accurate tool for drought monitoring, particularly in regions with complex environmental conditions. The strong correlation with VHI across different climates and seasons underscores its potential for broader application in North Africa and beyond.

3.5. Discussion

The validation of the Genetic Algorithm Optimized Multispectral Soil-Vegetation Drought Index (GA-MSVDI) against traditional drought indices, such as the VHI, has demonstrated the robustness and reliability of the new index across diverse climatic regions in North Africa. The GA-MSVDI consistently exhibited high correlation values with VHI, particularly in the Nile Delta and El Kairouan regions, indicating its strong potential for accurate drought monitoring in regions characterized by significant agricultural activities and variable climatic conditions.

Unlike other traditional drought indices which apply fixed empirical weightings, GA-MSVDI applies a Genetic Algorithm-based optimization method to dynamically weigh the contribution of different satellite-derived indices. This offers greater flexibility under different climatic conditions. GA-MSVDI also employs multi-source high-resolution satellite data (S1, S2, and Landsat-8), whereas most existing studies employ coarser-resolution data such as MODIS or AVHRR. This improvement enhances spatial

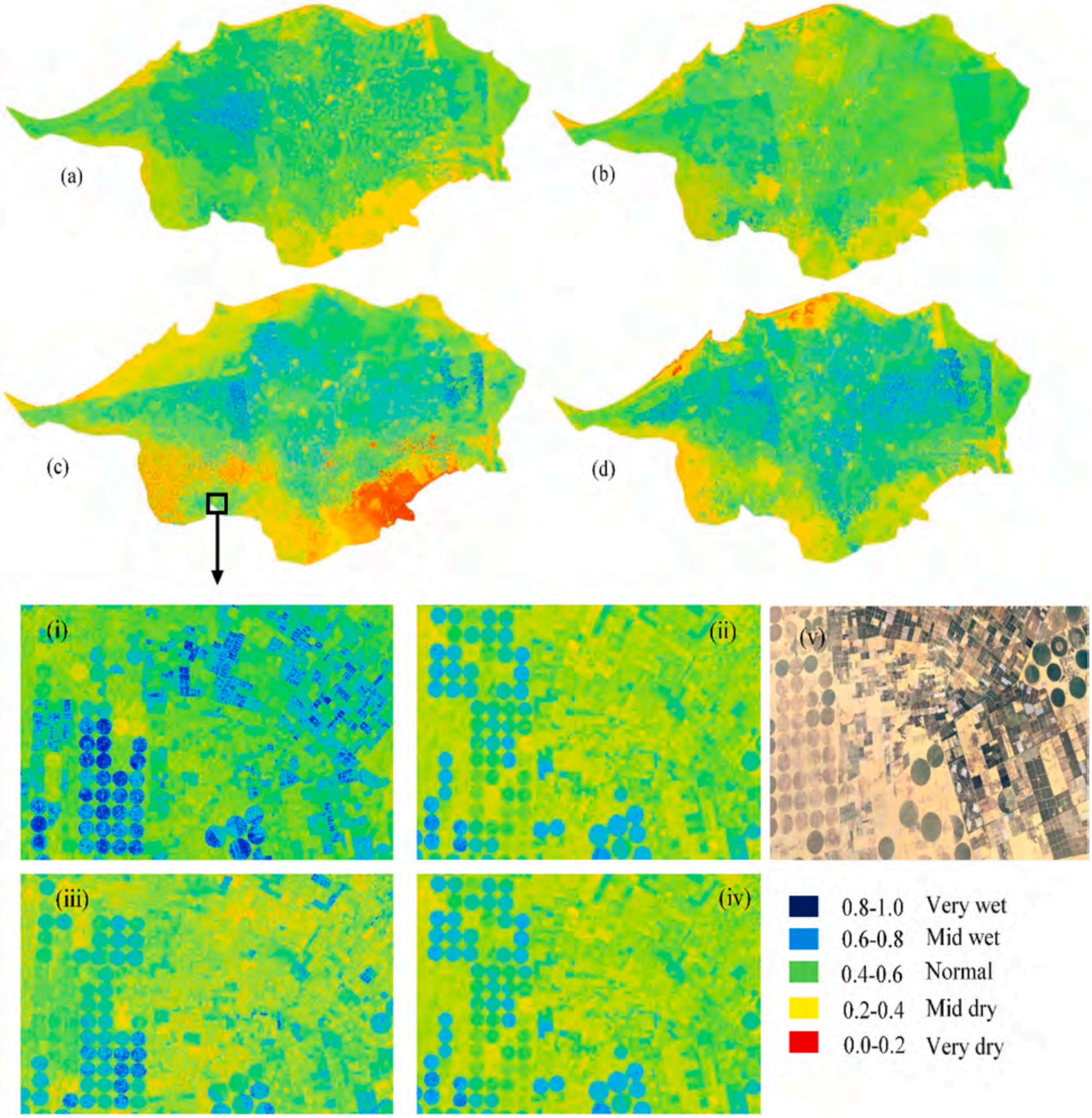

Fig. 10. Drought map at Nile delta in Egypt (a) Jan to Mar (b) Apr to Jun (c) Jul to Sep (d) Oct to Dec (i) subset Jan to Mar (ii) subset Apr to Jun (iii) subset Jul to Sep (iv) subset Oct to Dec (v) google earth very high-resolution image of subset.

precision and drought identification, particularly in heterogeneous agricultural landscapes. GA-MSVDI consistently outperforms the traditional indices in the identification of drought in all study areas and seasons. In the Nile Delta, GA-MSVDI was top-ranked in correlation with VHI (0.74–0.91) ahead of NDVI (0.69–0.80), TCI (0.68–0.81), VCI (0.67–0.79), and SWCI (0.65–0.72). This trend was mirrored in El Kairouan, where GA-MSVDI correlations (0.82–0.85) were greater than NDVI (0.71–0.81) and TCI (0.69–0.79).

In Rabat-Salé-Kénitra, GA-MSVDI varied seasonally (0.57–0.88) but was still superior to NDVI (0.63–0.79) and SWCI (0.62–0.74). Surprisingly, SWCI and VCI consistently showed inferior performance ($\leq$0.75) across all regions. The results confirm the higher precision and adaptability of GA-MSVDI as a more reliable tool for precision agriculture and drought monitoring over conventional indices.

The superior performance of GA-MSVDI can be attributed to its optimized weighting scheme, which emphasizes the combined importance of SMI and NDII. These components collectively accounted for a weight of 0.39, highlighting the critical role of soil moisture and vegetation water content in accurately detecting drought conditions.

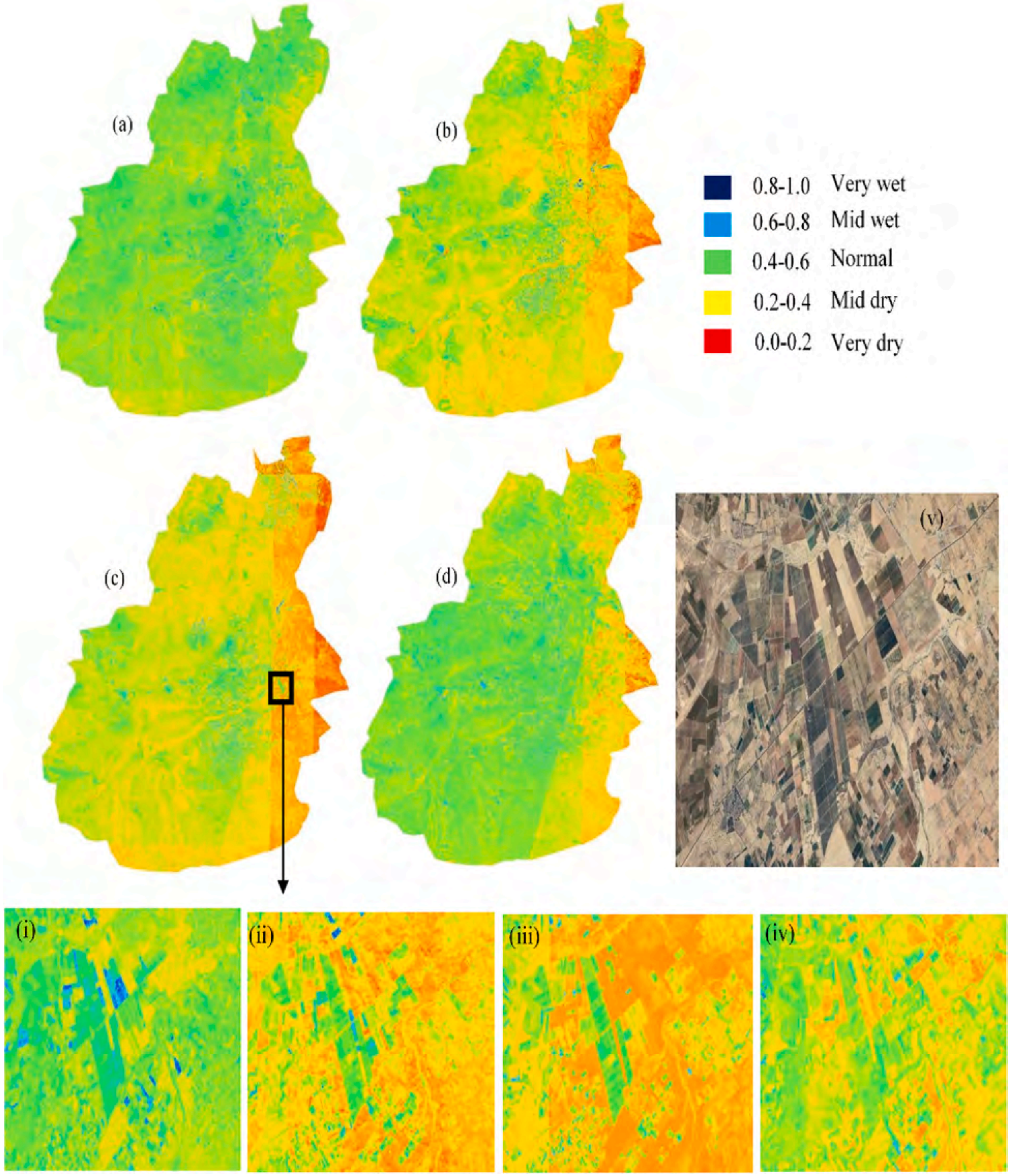

Fig. 11. Drought map at El Kairouan and its environs in Tunisia (a) Jan to Mar (b) Apr to Jun (c) Jul to Sep (d) Oct to Dec (i) subset Jan to Mar (ii) subset Apr to Jun (iii) subset Jul to Sep (iv) subset Oct to Dec (v) google earth very high-resolution image of subset.

With satellite-derived, high-resolution drought estimates, the GA-MSVDI enables policymakers to make better decisions for effective water allocation and saving. Its integration into national drought monitoring networks can provide early warning systems, allowing the authorities to implement proactive steps for the mitigation of agricultural losses and water deficits. The ability of GA-MSVDI to detect spatiotemporal variations in drought can make it an invaluable resource for the enhancement of irrigation

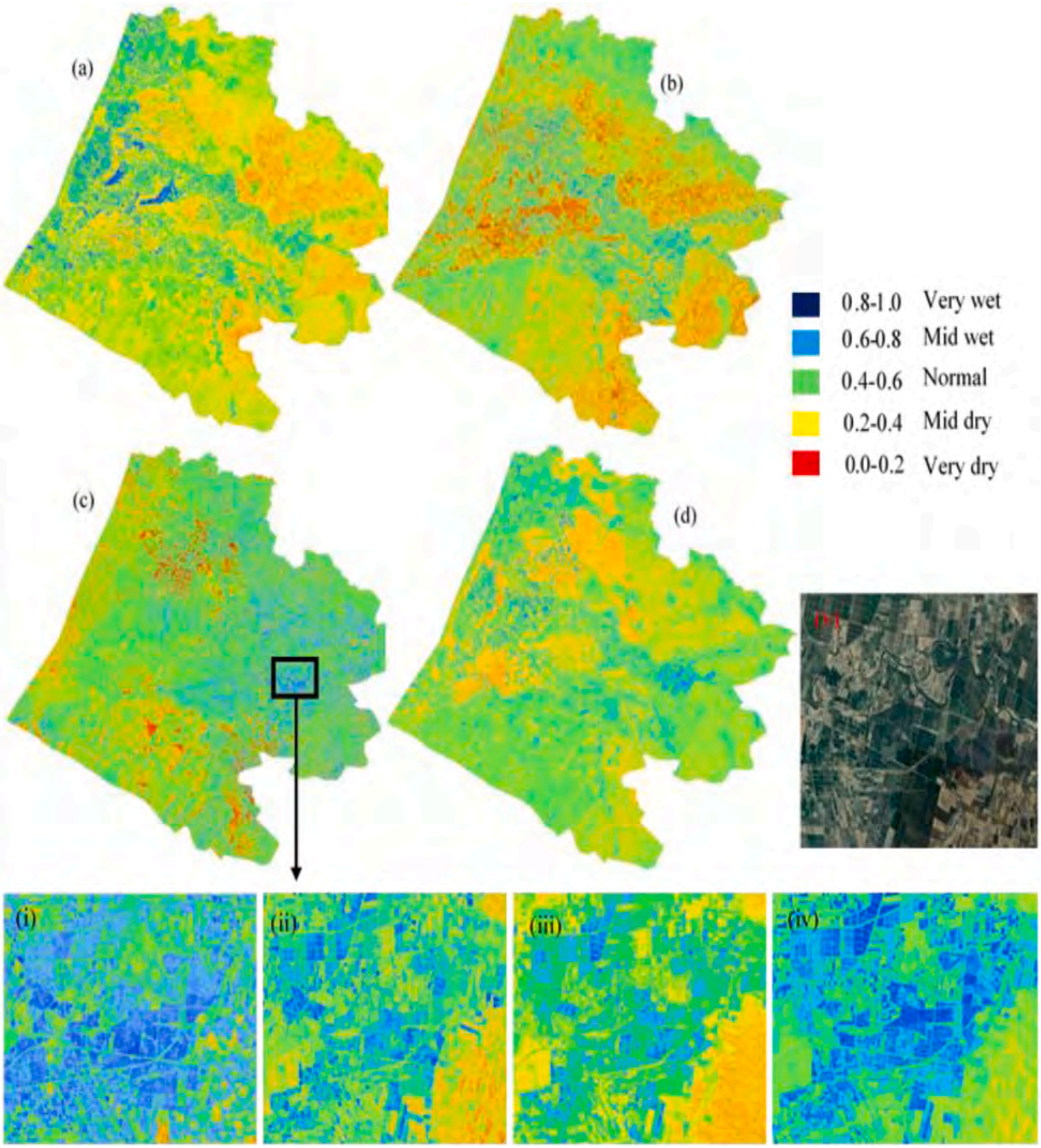

Fig. 12. Drought map Rabat-Salé-Kénitra in Morocco (a) Jan to Mar (b) Apr to Jun (c) Jul to Sep (d) Oct to Dec (i) subset Jan to Mar (ii) subset Apr to Jun (iii) subset Jul to Sep (iv) subset Oct to Dec (v) google earth very high-resolution image of subset.

techniques, crop yield optimization, and empowering climate adaptation policy. Agriculturally, farmers can use this index to enhance water use efficiency, minimize yield loss, and adopt sustainable agricultural production strategies responsive to real-time drought conditions. Furthermore, the responsiveness of GA-MSVDI makes it compatible with conventional hydrological models and early warning systems, giving added strength to desertification control campaigns and food scarcity in vulnerable regions. Through bridging the gap between policy practice in the real world and remote sensing technology, GA-MSVDI can become a platform on which sustainable management of drought can occur, ensuring decision-makers are equipped with the capabilities required to reduce climate risks and ensure agricultural productivity.

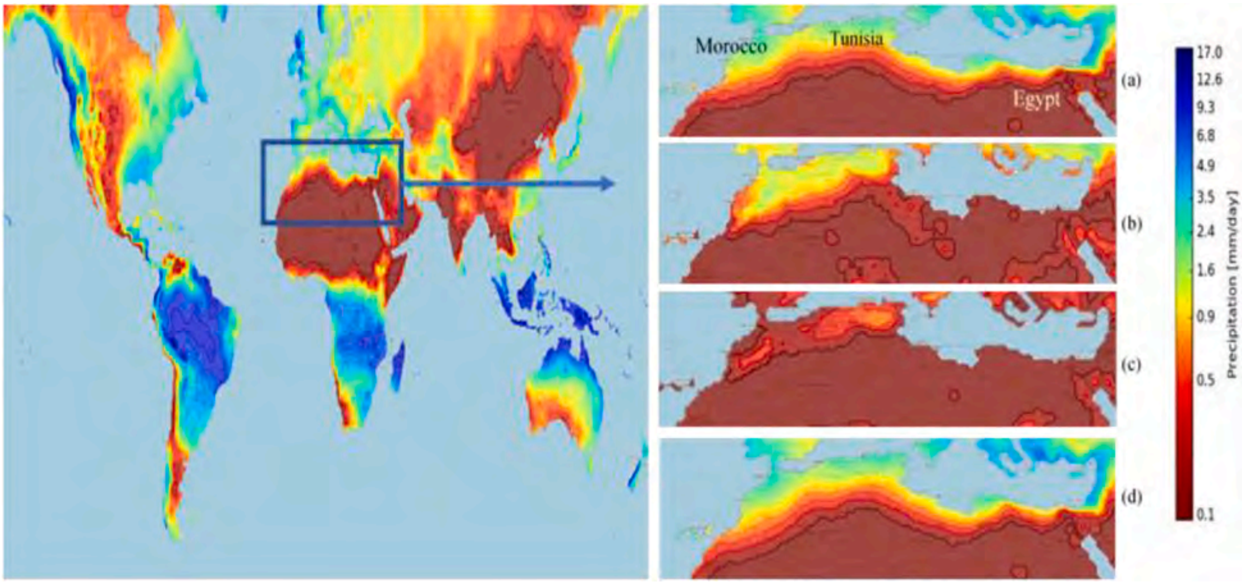

Fig. 13. Precipitation rate at the three study areas, accessed on August 24, 2024, at climatemaps.romgens.com, (a) January, (b) May, (c) August, (d) November.

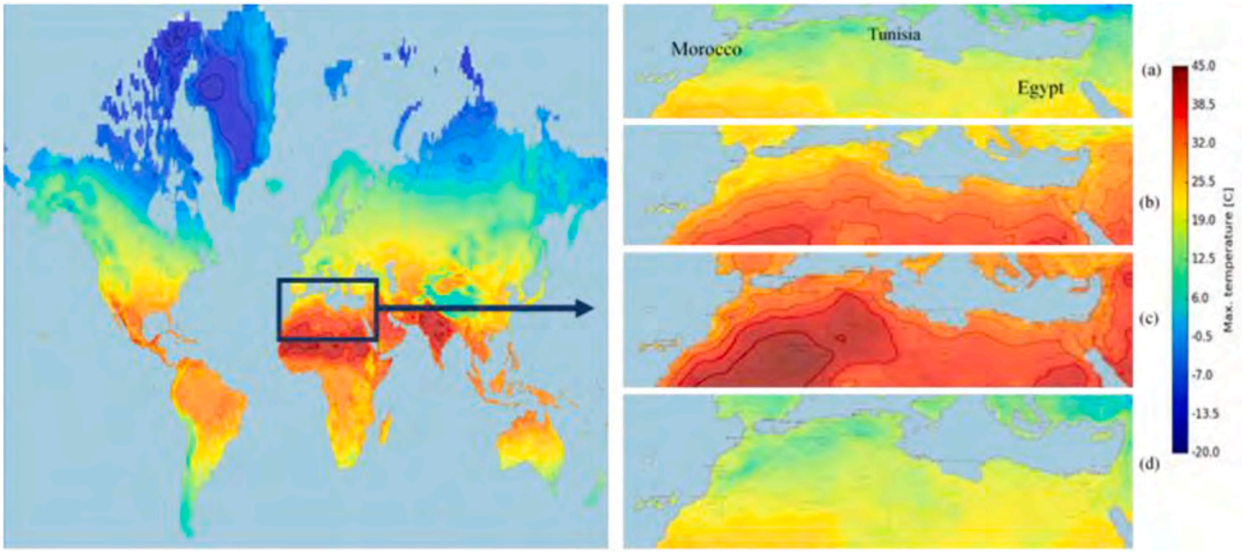

Fig. 14. Max temperature distribution at the three study areas, accessed on August 24, 2024, at climatemaps.romgens.com, (a) January, (b) May, (c) August, (d) November.

However, despite these promising results, certain limitations must be acknowledged. One of the primary challenges lies in the variability of GA-MSVDI's performance across different regions, as observed in the Rabat-Salé-Kénitra region of Morocco. The index's slightly lower correlation during certain periods could be influenced by the complex interplay of climatic factors, land use, and agricultural practices that are not fully captured by the current set of indices. Satellite datasets have uncertainties underpinning by sensor calibration error and atmospheric perturbation, potentially affecting accuracy. Cloud cover creates issues for optical sensors like Sentinel-2 and Landsat-8, potentially causing data gaps, though Sentinel-1 SAR diminishes it somewhat. Temporal resolution inconsistencies among sensors may affect consistency in drought monitoring, and ground-truth verification is constrained by paucity of meteorological observations in certain areas. Moreover, the Genetic Algorithm (GA) is computationally demanding, consuming large amounts of processing power, which could restrict real-time uses unless optimized for performance. Redressing these will further improve the reliability and scalability of GA-MSVDI.

Further studies ought to concentrate on improving the GA-MSVDI by incorporating additional environmental variables that may further enhance its accuracy and applicability across different climatic zones. The inclusion of more localized climatic data, such as soil temperature and humidity, could offer a more complex comprehension of the dynamics of drought. Additionally, expanding the validation process to include longer time series data and more diverse geographical regions will be essential for assessing the long-term reliability of the index. Exploring machine learning techniques to dynamically adjust the index weights based on real-time data could also enhance its adaptability and precision in drought monitoring.

4. Conclusion

GA-MSVDI presents a quantum leap in the effort of agricultural drought monitoring. With smart integration of high-resolution satellite data from S1, S2, and Landsat-8, the GA-MSVDI captures the synergy of soil moisture, vegetation health, and temperature that significantly tops the relevance criteria of any drought index. The optimization process, which assigns the most appropriate weights to each index, ensures that the GA-MSVDI is not only responsive to the unique climatic conditions of North Africa but also highly reliable across diverse agricultural landscapes.

The index's performance, as validated against the VHI, underscores its robustness and precision, with strong correlations observed across different study regions. This validation, coupled with the index's capacity to reflect real-time drought dynamics, marks a substantial improvement over traditional indices, offering a more nuanced and effective tool for drought management. GA-MSVDI is highly correlated with commonly applied drought indices (0.57–0.91), confirming its ability to measure drought severity precisely. Its robustness in different geographical settings, including Mediterranean and semi-arid environments, demonstrates its flexibility and reliability in different environments. By combining high-resolution satellite data (S1, S2, and Landsat-8) and Genetic Algorithm optimization, GA-MSVDI provides an improved drought monitoring system compared to traditional indices. Its ability to sense soil wetness, plant health, and temperatures makes it particularly valuable for precision agriculture so that efficient irrigation, pre-drought mitigation, and improved resource use in water-constrained environments can be achieved.

The GA-MSVDI belongs to some of the state-of-the-art powerful tools that promise a radical revolution in drought monitoring and management. With the capacity for high-resolution accuracy, it becomes an incredible tool in building agricultural resilience for food security in the face of an utterly unpredictable climate. The GA-MSVDI would, therefore, form one of the cornerstones in environmental monitoring, critical for long-term planning and support of sustainable agriculture practices.

CRediT authorship contribution statement

Nasser A.M. Abdelrahim: Writing – original draft, Visualization, Validation, Resources, Methodology, Formal analysis, Data curation, Conceptualization. **Shuanggen Jin:** Writing – review & editing, Supervision, Software, Project administration, Investigation, Funding acquisition.

Ethical statement

We, the authors, hereby confirm that our research meets the highest ethical standards as outlined in the guidelines of Remote Sensing Applications: Society and Environment. This manuscript is an original work, with data collected and analyzed in a transparent and accurate manner. Further, the methods utilized ensure that the privacy and well-being of human populations and the environment are duly protected, with proper approvals acquired whenever appropriate. There are no conflicts of interest to declare that could have biased the findings presented in this study, and we have made the necessary acknowledgments of all contributors. We intend to share our data according to the principles of open science and are committed to responsible dissemination of our work for societal and environmental benefit.

Funding

This work was supported by the Henan International Science and Technology Cooperation Key Project (Grant No. 241111520700), Henan Department of Education's "Double First-Class" Project (Grant No. 760507/033) and Henan Polytechnic University Startup Foundation Project (Grant No. 722403/067/002).

Declaration of competing interest

The authors declare the following financial interests/personal relationships which may be considered as potential competing interests: Nasser A. M. Abdelrahim reports administrative support was provided by Henan International Science and Technology Cooperation Key Project. If there are other authors, they declare that they have no known competing financial interests or personal relationships that could have appeared to influence the work reported in this paper.

Acknowledgement

The authors would like to thank NASA for providing Landsat-8 data and ESA for providing the Sentinel-1 and Sentinel-2data used in this article.

Data availability

Data will be made available on request.

References

Abdelrahim, N.A.M., Jin, S., 2025. A novel Agricultural Remote Sensing Srought Index (ARSDI) for high-resolution drought assessment in Africa using sentinel and landsat data. Environ. Monit. Assess. 197, 242. https://doi.org/10.1007/s10661-025-13686-3.

Abdulmana, S., Lim, A., Wongsai, S., Wongsai, N., 2021. Land surface temperature and vegetation cover changes and their relationships in Taiwan from 2000 to 2020. Remote Sens. Appl.: Soc. Environ. 24, 100636. https://doi.org/10.1016/j.rsase.2021.100636.

Afshar, M.H., Al-Yaari, A., Yilmaz, M.T., 2021. Comparative evaluation of microwave L-band VOD and optical NDVI for agriculture drought detection over Central Europe. Remote Sens. 13, 1251. https://doi.org/10.3390/rs13071251.

Al Saud, M.M. (Ed.), 2022. Applications of Space Techniques on the Natural Hazards in the MENA Region. Springer International Publishing, Cham. https://doi.org/10.1007/978-3-030-88874-9.

Alahacoon, N., Edirisinghe, M., 2022. A comprehensive assessment of remote sensing and traditional based drought monitoring indices at global and regional scale. Geomat. Nat. Hazards Risk 13, 762–799. https://doi.org/10.1080/19475705.2022.2044394.

Alahacoon, N., Edirisinghe, M., Ranagalage, M., 2021. Satellite-based meteorological and agricultural drought monitoring for agricultural sustainability in Sri Lanka. Sustainability 13, 3427. https://doi.org/10.3390/su13063427.

Amiri, N., Lahlali, R., Amiri, S., El Jarroudi, M., Khebiza, M.Y., Messouli, M., 2021. Development of an integrated model to assess the impact of agricultural practices and land use on agricultural production in Morocco under climate stress over the next Twenty Years. Sustainability 13, 11943. https://doi.org/10.3390/su132111943.

Arabi Aliabad, F., Zare, M., Ghafarian Malamiri, H., Ghaderpour, E., 2023. Improving the accuracy of landsat 8 land surface temperature in arid regions by MODIS water vapor imagery. Atmosphere 14, 1589. https://doi.org/10.3390/atmos14101589.

Araneda-Cabrera, R.J., Bermúdez, M., Puertas, J., 2021. Benchmarking of drought and climate indices for agricultural drought monitoring in Argentina. Sci. Total Environ. 790, 148090. https://doi.org/10.1016/j.scitotenv.2021.148090.

Atzberger, C., 2013. Advances in remote sensing of agriculture: context description, existing operational monitoring systems and major information needs. Remote Sens. 5, 949–981. https://doi.org/10.3390/rs5020949.

Ayyad, S., Al Zayed, I.S., Ha, V.T.T., Ribbe, L., 2019. The performance of satellite-based actual evapotranspiration products and the assessment of irrigation efficiency in Egypt. Water 11, 1913. https://doi.org/10.3390/w11091913.

Bayissa, Y., Maskey, S., Tadesse, T., Van Andel, S., Moges, S., Van Griensven, A., Solomatine, D., 2018. Comparison of the performance of six drought indices in characterizing historical drought for the upper blue Nile Basin, Ethiopia. Geosciences 8, 81. https://doi.org/10.3390/geosciences8030081.

Begum, M.S., Bala, S.K., Islam, A.S., Islam, G.T., Roy, D., 2021. An analysis of spatio-temporal trends of land surface temperature in the Dhaka Metropolitan area by applying landsat images. JGIS 13, 538–560. https://doi.org/10.4236/jgis.2021.134030.

Behnassi, M., Barjees Baig, M., El Haiba, M., Reed, M.R. (Eds.), 2021. Emerging Challenges to Food Production and Security in Asia, Middle East, and Africa: Climate Risks and Resource Scarcity. Springer International Publishing, Cham. https://doi.org/10.1007/978-3-030-72987-5.

Bento, V.A., Gouveia, C.M., DaCamara, C.C., Trigo, I.F., 2018. A climatological assessment of drought impact on vegetation health index. Agric. For. Meteorol. 259, 286–295. https://doi.org/10.1016/j.agrformet.2018.05.014.

Bento, V.A., Gouveia, C.M., DaCamara, C.C., Libonati, R., Trigo, I.F., 2020. The roles of NDVI and land surface temperature when using the vegetation health index over dry regions. Global Planet. Change 190, 103198. https://doi.org/10.1016/j.gloplacha.2020.103198.

Bhogapurapu, N., Dey, S., Homayouni, S., Bhattacharya, A., Rao, Y.S., 2022a. Field-scale soil moisture estimation using sentinel-1 GRD SAR data. Adv. Space Res. 70, 3845–3858. https://doi.org/10.1016/j.asr.2022.03.019.

Bhogapurapu, N., Dey, S., Mandal, D., Bhattacharya, A., Karthikeyan, L., McNairn, H., Rao, Y.S., 2022b. Soil moisture retrieval over croplands using dual-pol L-band GRD SAR data. Rem. Sens. Environ. 271, 112900. https://doi.org/10.1016/j.rse.2022.112900.

Bhuiyan, C., Singh, R.P., Kogan, F.N., 2006. Monitoring drought dynamics in the Aravalli Region (India) using different indices based on ground and remote sensing data. Int. J. Appl. Earth Obs. Geoinf. 8, 289–302. https://doi.org/10.1016/j.jag.2006.03.002.

Bhuyan-Erhardt, U., Erhardt, T.M., Laaha, G., Zang, C., Parajka, J., Menzel, A., 2019. Validation of drought indices using environmental indicators: streamflow and carbon flux data. Agric. For. Meteorol. 265, 218–226. https://doi.org/10.1016/j.agrformet.2018.11.016.

Binte Mostafiz, R., Noguchi, R., Ahamed, T., 2021. Agricultural land suitability assessment using satellite remote sensing-derived soil-vegetation indices. Land 10, 223. https://doi.org/10.3390/land10020223.

Brandt, M., Hiernaux, P., Rasmussen, K., Mbow, C., Kergoat, L., Tagesson, T., Ibrahim, Y.Z., Wélé, A., Tucker, C.J., Fensholt, R., 2016. Assessing woody vegetation trends in Sahelian Drylands using MODIS based seasonal metrics. Rem. Sens. Environ. 183, 215–225. https://doi.org/10.1016/j.rse.2016.05.027.

Brown, J.F., Pervez, M.S., 2014. Merging remote sensing data and national agricultural statistics to model change in irrigated agriculture. Agric. Syst. 127, 28–40. https://doi.org/10.1016/j.agsy.2014.01.004.

Chaudhary, S.K., Srivastava, P.K., Gupta, D.K., Kumar, P., Prasad, R., Pandey, D.K., Das, A.K., Gupta, M., 2022. Machine learning algorithms for soil moisture estimation using Sentinel-1: model development and implementation. Adv. Space Res. 69, 1799–1812. https://doi.org/10.1016/j.asr.2021.08.022.

Chen, N., Yu, L., Zhang, X., Shen, Y., Zeng, L., Hu, Q., Niyogi, D., 2020. Mapping paddy rice fields by combining multi-temporal vegetation index and synthetic aperture radar remote sensing data using google earth engine machine learning platform. Remote Sens. 12, 2992. https://doi.org/10.3390/rs12182992.

Chen, M., Yu, L., Zhi, C., Sun, R., Zhu, S., Gao, Z., Ke, Z., Zhu, M., Zhang, Y., 2022. Improved faster R-CNN for fabric defect detection based on Gabor filter with Genetic Algorithm optimization. Comput. Ind. 134, 103551. https://doi.org/10.1016/j.compind.2021.103551.

Chen, D., Hu, H., Liao, C., Ye, J., Bao, W., Mo, J., Wu, Y., Dong, T., Fan, H., Pei, J., 2023. Crop NDVI time series construction by fusing Sentinel-1, Sentinel-2, and environmental data with an ensemble-based framework. Comput. Electron. Agric. 215, 108388. https://doi.org/10.1016/j.compag.2023.108388.

Corbari, C., Paciolla, N., Restuccia, G., Al Bitar, A., 2024. Multi-scale EO-based agricultural drought monitoring indicator for operative irrigation networks management in Italy. J. Hydrol.: Reg. Stud. 52, 101732. https://doi.org/10.1016/j.ejrh.2024.101732.

Dai, A., 2011. Drought under global warming: a review. WIREs Climate Change 2, 45–65. https://doi.org/10.1002/wcc.81.

Dey, N. (Ed.), 2023. Applied Genetic Algorithm and its Variants: Case Studies and New Developments, Springer Tracts in Nature-Inspired Computing. Springer Nature Singapore, Singapore. https://doi.org/10.1007/978-981-99-3428-7.

Dong, J., Xing, L., Cui, N., Zhao, L., Guo, L., Gong, D., 2023. Standardized Precipitation Evapotranspiration Index (SPEI) estimated using variant long short-term memory network at four climatic zones of China. Comput. Electron. Agric. 213, 108253. https://doi.org/10.1016/j.compag.2023.108253.

Dos Santos Araujo, D.C., Gico Lima Montenegro, S.M., Ribeiro Neto, A., Da Silva, S.F., 2024. Evaluation of satellite-based soil moisture for agricultural drought monitoring in the Brazilian Semiarid Region. Remote Sens. Appl.: Soc. Environ. 33, 101111. https://doi.org/10.1016/j.rsase.2023.101111.

Dotzler, S., Hill, J., Buddenbaum, H., Stoffels, J., 2015. The potential of EnMAP and sentinel-2 data for detecting drought stress phenomena in deciduous forest communities. Remote Sens. 7, 14227–14258. https://doi.org/10.3390/rs71014227.

Edokossi, K., Calabia, A., Jin, S., Molina, I., 2020. GNSS-reflectometry and remote sensing of soil moisture: a review of measurement techniques, methods, and applications. Remote Sens. 12, 614. https://doi.org/10.3390/rs12040614.

Edokossi, K., Jin, S., Calabia, A., Molina, I., Mazhar, U., 2024. Evaluation of SMAP and CYGNSS soil moistures in drought prediction using multiple linear regression and GLDAS product. Photogramm. Eng. Rem. Sens. 90, 303–312.

Elameen, A.M., Jin, S., Olago, D., 2023. Identification of drought events in major basins of Africa from GRACE total water storage and modeled products. Photogramm. Eng. Rem. Sens. 89, 221–232.

Esfahanian, E., Nejadhashemi, A.P., Abouali, M., Daneshvar, F., Alireza, A.R., Herman, M.R., Tang, Y., 2016. Defining drought in the context of stream health. Ecol. Eng. 94, 668–681. https://doi.org/10.1016/j.ecoleng.2016.06.110.

Esfahanian, E., Nejadhashemi, A.P., Abouali, M., Adhikari, U., Zhang, Z., Daneshvar, F., Herman, M.R., 2017. Development and evaluation of a comprehensive drought index. J. Environ. Manag. 185, 31–43. https://doi.org/10.1016/j.jenvman.2016.10.050.

Ewis Omran, E.-S., Negm, A.M. (Eds.), 2020. Climate Change Impacts on Agriculture and Food Security in Egypt: Land and Water Resources—Smart Farming—Livestock, Fishery, and Aquaculture. Springer International Publishing, Cham. https://doi.org/10.1007/978-3-030-41629-4. Springer Water.

Farrag, A., Mostafa, Y., Abdelrahim, N., 2020. Detecting land cover changes using vhr satellite images: a comparative study. JES. J. Eng. Sci. 48, 200–211. https://doi.org/10.21608/jesaun.2019.264927.

Felegari, S., Sharifi, A., Moravej, K., Amin, M., Golchin, A., Muzirafuti, A., Tariq, A., Zhao, N., 2021. Integration of sentinel 1 and sentinel 2 satellite images for crop mapping. Appl. Sci. 11, 10104. https://doi.org/10.3390/app112110104.

Fensholt, R., Sandholt, I., 2003. Derivation of a shortwave infrared water stress index from MODIS near- and shortwave infrared data in a semiarid environment. Rem. Sens. Environ. 87, 111–121. https://doi.org/10.1016/j.rse.2003.07.002.

Foucras, M., Zribi, M., Albergel, C., Baghdadi, N., Calvet, J.-C., Pellarin, T., 2020. Estimating 500-m resolution soil moisture using sentinel-1 and optical data synergy. Water 12, 866. https://doi.org/10.3390/w12030866.

Gaber, Y., Ahmed, N., Ali Farrag, F., 2021. Change detection for map updating using very high resolution satellite images. JES. J. Eng. Sci. 424–445. https://doi.org/10.21608/jesaun.2021.67949.1039, 0.

Gad, A.F., 2023. PyGAD: an intuitive genetic algorithm Python library. Multimed. Tool. Appl. 83, 58029–58042. https://doi.org/10.1007/s11042-023-17167-y.

González-Gómez, L., Intrigliolo, D.S., Rubio-Asensio, J.S., Buesa, I., Ramírez-Cuesta, J.M., 2022. Assessing almond response to irrigation and soil management practices using vegetation indexes time-series and plant water status measurements. Agric. Ecosyst. Environ. 339, 108124. https://doi.org/10.1016/j.agee.2022.108124.

Hao, Z., AghaKouchak, A., 2014. A nonparametric multivariate multi-index drought monitoring framework. J. Hydrometeorol. 15, 89–101. https://doi.org/10.1175/JHM-D-12-0160.1.

Hao, Z., Singh, V.P., 2015. Drought characterization from a multivariate perspective: a review. J. Hydrol. 527, 668–678. https://doi.org/10.1016/j.jhydrol.2015.05.031.

Hao, C., Zhang, J., Yao, F., 2015. Combination of multi-sensor remote sensing data for drought monitoring over Southwest China. Int. J. Appl. Earth Obs. Geoinf. 35, 270–283. https://doi.org/10.1016/j.jag.2014.09.011.

Hayes, M., Svoboda, M., Wall, N., Widhalm, M., 2011. The lincoln declaration on drought indices: Universal meteorological drought index recommended. Bull. Am. Meteorol. Soc. 92 (1), 485–488. https://doi.org/10.1175/2010BAMS3103.

Hayes, M.J., Svoboda, M.D., Wardlow, B.D., Anderson, M.C., Kogan, F., 2012. Drought Monitoring: Historical and Current Perspectives.

Hazaymeh, K., Hassan, Q.K., 2017. A remote sensing-based agricultural drought indicator and its implementation over a semi-arid region. Jordan. J. Arid Land 9, 319–330. https://doi.org/10.1007/s40333-017-0014-6.

Heim, R.R.H., 2002. A Review of Twentieth- Century Drought Indices Used in the United States.

Holben, B.N., 1980. Spectral Assessment of Soybean Leaf Area and Leaf Biomass. PHOTOGRAMMETRIC ENGINEERING.

Huete, A.R., 1988. A Soil-Adjusted Vegetation Index (SAVI). Rem. Sens. Environ. 25, 295–309. https://doi.org/10.1016/0034-4257(88)90106-X.

Jiao, W., Zhang, L., Chang, Q., Fu, D., Cen, Y., Tong, Q., 2016. Evaluating an enhanced Vgetation Condition Index (VCI) based on VIUPD for drought monitoring in the continental United States. Remote Sens. 8, 224. https://doi.org/10.3390/rs8030224.

Jiao, W., Tian, C., Chang, Q., Novick, K.A., Wang, L., 2019. A new multi-sensor integrated index for drought monitoring. Agric. For. Meteorol. 268, 74–85. https://doi.org/10.1016/j.agrformet.2019.01.008.

Jin, S., Zhang, T., 2016. Terrestrial water storage anomalies associated with drought in Southwestern USA from GPS observations. Surv. Geophys. 37, 1139–1156. https://doi.org/10.1007/s10712-016-9385-z.

Jin, S., Wang, Q., Dardanelli, G., 2022. A review on multi-GNSS for earth observation and emerging applications. Remote Sens. 14, 3930. https://doi.org/10.3390/rs14163930.

Jin, S., Camps, A., Jia, Y., Wang, F., Martin-Neira, M., Huang, F., Yan, Q., Zhang, S., Li, Z., Edokossi, K., Yang, D., Xiao, Z., Ma, Z., Bai, W., 2024. Remote sensing and its applications using GNSS reflected signals: advances and prospects. Satell Navig 5, 19. https://doi.org/10.1186/s43020-024-00139-4.

Kaiser, P., Buddenbaum, H., Nink, S., Hill, J., 2022. Potential of sentinel-1 data for spatially and temporally high-resolution detection of drought affected forest stands. Forests 13, 2148. https://doi.org/10.3390/f13122148.

Katoch, S., Chauhan, S.S., Kumar, V., 2021. A review on genetic algorithm: past, present, and future. Multimed. Tool. Appl. 80, 8091–8126. https://doi.org/10.1007/s11042-020-10139-6.

Kaur, A., Sood, S.K., 2020. Cloud-Fog based framework for drought prediction and forecasting using artificial neural network and genetic algorithm. J. Exp. Theor. Artif. Intell. 32, 273–289. https://doi.org/10.1080/0952813X.2019.1647563.

Kogan, Felix N., 1995. Droughts of the late 1980s in the United States as derived from NOAA Polar-orbiting satellite data. Bull. Am. Meteorol. Soc. 76 (2), 655–668. https://doi.org/10.1175/1520-0477(1995)076<0655:DOTLIT>2.0.CO.

Kogan, F.N., 1997. Global drought watch from space. Bull. Am. Meteorol. Soc. 78, 621–636. https://doi.org/10.1175/1520-0477(1997)078<0621:GDWFS>2.0.CO, 2.

Konno, T., Homma, K., 2023. Prediction of areal soybean lodging using a main stem elongation model and a soil-adjusted vegetation index that accounts for the ratio of vegetation cover. Remote Sens. 15, 3446. https://doi.org/10.3390/rs15133446.

Li, L., Cai, H., 2024. A comparative study of various drought indices at different timescales and over different record lengths in the arid area of Northwest China. Environ. Sci. Pollut. Res. 31, 25096–25113. https://doi.org/10.1007/s11356-024-32803-2.

Li, H., Yin, Y., Zhou, J., Li, F., 2024. Improved agricultural drought monitoring with an integrated drought condition index in Xinjiang. China. Water 16, 325. https://doi.org/10.3390/w16020325.

Malakar, N.K., Hulley, G.C., 2016. A water vapor scaling model for improved land surface temperature and emissivity separation of MODIS thermal infrared data. Rem. Sens. Environ. 182, 252–264. https://doi.org/10.1016/j.rse.2016.04.023.

Mathivha, F., Mbatha, N., 2021. Comparison of long-term changes in non-linear aggregated drought index calibrated by MERRA–2 and NDII soil moisture proxies. Water 14, 26. https://doi.org/10.3390/w14010026.

Mbatha, N., Xulu, S., 2018. Time series analysis of MODIS-derived NDVI for the hluhluwe-imfolozi Park, South Africa: impact of recent intense drought. Climate 6, 95. https://doi.org/10.3390/cli6040095.

Mishra, A., Vu, T., Veettil, A.V., Entekhabi, D., 2017. Drought monitoring with Soil Moisture Active Passive (SMAP) measurements. J. Hydrol. 552, 620–632. https://doi.org/10.1016/j.jhydrol.2017.07.033.

Moursy, M.A.M., ElFetyany, M., Meleha, A.M.I., El-Bialy, M.A., 2023. Productivity and profitability of modern irrigation methods through the application of on-farm drip irrigation on some crops in the Northern Nile Delta of Egypt. Alex. Eng. J. 62, 349–356. https://doi.org/10.1016/j.aej.2022.06.063.

Mullissa, A., Vollrath, A., Odongo-Braun, C., Slagter, B., Balling, J., Gou, Y., Gorelick, N., Reiche, J., 2021. Sentinel-1 SAR backscatter analysis ready data preparation in google earth engine. Remote Sens. 13, 1954. https://doi.org/10.3390/rs13101954.

Najibi, N., Jin, S., 2013. Physical reflectivity and polarization characteristics for snow and ice-covered surfaces interacting with GPS signals. Remote Sens. 5, 4006–4030. https://doi.org/10.3390/rs5084006.

Pande, C.B., Moharir, K.N., Singh, S.K., Pham, Q.B., Elbeltagi, A. (Eds.), 2023. Climate Change Impacts on Natural Resources, Ecosystems and Agricultural Systems. Springer Climate. Springer International Publishing, Cham. https://doi.org/10.1007/978-3-031-19059-9.

Palmer, W.C., 1965. Meteorological Drought. US Department of Commerce, Weather Bureau.

Pande, C.B., Egbueri, J.C., Costache, R., Sidek, L.M., Wang, Q., Alshehri, F., Din, N.M., Gautam, V.K., Chandra Pal, S., 2024. Predictive modeling of Land Surface Temperature (LST) based on Landsat-8 satellite data and machine learning models for sustainable development. J. Clean. Prod. 444, 141035. https://doi.org/10.1016/j.jclepro.2024.141035.

Pei, F., Wu, C., Liu, X., Li, X., Yang, K., Zhou, Y., Wang, K., Xu, L., Xia, G., 2018. Monitoring the vegetation activity in China using vegetation health indices. Agric. For. Meteorol. 248, 215–227. https://doi.org/10.1016/j.agrformet.2017.10.001.

Pervez, M.S., Brown, J.F., 2010. Mapping irrigated lands at 250-m scale by merging MODIS data and national agricultural statistics. Remote Sens. 2, 2388–2412. https://doi.org/10.3390/rs2102388.

Qin, Q., Wu, Z., Zhang, T., Sagan, V., Zhang, Z., Zhang, Y., Zhang, C., Ren, H., Sun, Y., Xu, W., Zhao, C., 2021. Optical and thermal remote sensing for monitoring agricultural drought. Remote Sens. 13, 5092. https://doi.org/10.3390/rs13245092.

Quiring, S.M., Ganesh, S., 2010. Evaluating the utility of the Vegetation Condition Index (VCI) for monitoring meteorological drought in Texas. Agric. For. Meteorol. 150, 330–339. https://doi.org/10.1016/j.agrformet.2009.11.015.

Razavi-Termeh, S.V., Sadeghi-Niaraki, A., Seo, M., Choi, S.-M., 2023. Application of genetic algorithm in optimization parallel ensemble-based machine learning algorithms to flood susceptibility mapping using radar satellite imagery. Sci. Total Environ. 873, 162285. https://doi.org/10.1016/j.scitotenv.2023.162285.

Ren, J., Shao, Y., Wan, H., Xie, Y., Campos, A., 2021. A two-step mapping of irrigated corn with multi-temporal MODIS and Landsat analysis ready data. ISPRS J. Photogrammetry Remote Sens. 176, 69–82. https://doi.org/10.1016/j.isprsjprs.2021.04.007.

Rhyma, P.P., Norizah, K., Hamdan, O., Faridah-Hanum, I., Zulfa, A.W., 2020. Integration of normalised different vegetation index and Soil-Adjusted Vegetation Index for mangrove vegetation delineation. Remote Sens. Appl.: Soc. Environ. 17, 100280. https://doi.org/10.1016/j.rsase.2019.100280.

Sakellariou, S., Spiliotopoulos, M., Alpanakis, N., Faraslis, I., Sidiropoulos, P., Tziatzios, G.A., Karoutsos, G., Dalezios, N.R., Dercas, N., 2024. Spatiotemporal drought assessment based on gridded Standardized Precipitation Index (SPI) in vulnerable agroecosystems. Sustainability 16, 1240. https://doi.org/10.3390/su16031240.

Salem, S., Gaagai, A., Ben Slimene, I., Moussa, A., Zouari, K., Yadav, K., Eid, M., Abukhadra, M., El-Sherbeeny, A., Gad, M., Farouk, M., Elsherbiny, O., Elsayed, S., Bellucci, S., Ibrahim, H., 2023. Applying multivariate analysis and machine learning approaches to evaluating groundwater quality on the Kairouan Plain, Tunisia. Water 15, 3495. https://doi.org/10.3390/w15193495.

Sánchez, N., González-Zamora, Á., Piles, M., Martínez-Fernández, J., 2016. A new soil moisture agricultural drought index (SMADI) integrating MODIS and SMOS products: a case of study over the Iberian Peninsula. Remote Sens. 8, 287. https://doi.org/10.3390/rs8040287.

Sardooi, E.R., Azareh, A., Damaneh, Hadi Eskandari, Damaneh, Hamed Eskandari, 2021. Drought monitoring using MODIS land surface temperature and normalized difference vegetation index products. In: Semi-Arid Areas of Iran 11.

Schilling, J., Hertig, E., Tramblay, Y., Scheffran, J., 2020. Climate change vulnerability, water resources and social implications in North Africa. Reg. Environ. Change 20, 15. https://doi.org/10.1007/s10113-020-01597-7.

Schwabe, K., Albiac, J., Connor, J.D., Hassan, R.M., Meza González, L. (Eds.), 2013. Drought in Arid and Semi-arid Regions: A Multi-Disciplinary and Cross-Country Perspective. Springer, Netherlands, Dordrecht. https://doi.org/10.1007/978-94-007-6636-5.

Shahzaman, M., Zhu, W., Bilal, M., Habtemicheal, B.A., Mustafa, F., Arshad, M., Ullah, I., Ishfaq, S., Iqbal, R., 2021. Remote sensing indices for spatial monitoring of agricultural drought in South Asian Countries. Remote Sens. 13, 2059. https://doi.org/10.3390/rs13112059.

Skakun, S., Kussul, N., Shelestov, A., Kussul, O., 2016. The use of satellite data for agriculture drought risk quantification in Ukraine. Geomat. Nat. Hazards Risk 7, 901–917. https://doi.org/10.1080/19475705.2015.1016555.

Sriwongsitanon, N., Gao, H., Savenije, H.H.G., Maekan, E., Saengsawang, S., Thianpopirug, S., 2016. Comparing the Normalized Difference Infrared Index (NDII) with root zonestorage in a lumped conceptual model. Hydrol. Earth Syst. Sci. 20, 3361–3377. https://doi.org/10.5194/hess-20-3361-2016.

Sudmanns, M., Tiede, D., Augustin, H., Lang, S., 2020. Assessing global Sentinel-2 coverage dynamics and data availability for operational Earth observation (EO) applications using the EO-Compass. Int. J.Digital Earth 13, 768–784. https://doi.org/10.1080/17538947.2019.1572799.

Tang, H., Li, Z.-L., 2014. Quantitative remote sensing in thermal infrared: theory and applications. Springer Remote Sensing/Photogrammetry. Springer, Berlin Heidelberg, Berlin, Heidelberg. https://doi.org/10.1007/978-3-642-42027-6.

Teluguntla, P., Thenkabail, P.S., Oliphant, A., Xiong, J., Gumma, M.K., Congalton, R.G., Yadav, K., Huete, A., 2018. A 30-m landsat-derived cropland extent product of Australia and China using random forest machine learning algorithm on Google Earth Engine cloud computing platform. ISPRS J. Photogrammetry Remote Sens. 144, 325–340. https://doi.org/10.1016/j.isprsjprs.2018.07.017.

Thenkabail, P.S., Ward, A.D., Lyon, J.G., 1994. Landsat-5 Thematic Mapper models of soybean and corn crop characteristics. Int. J. Rem. Sens. 15, 49–61. https://doi.org/10.1080/01431169408954050.

Tian, L., Yuan, S., Quiring, S.M., 2018. Evaluation of six indices for monitoring agricultural drought in the south-central United States. Agric. For. Meteorol. 249, 107–119. https://doi.org/10.1016/j.agrformet.2017.11.024.

Tran, Hoa Thi, Campbell, J.B., Tran, T.D., Tran, Ha Thanh, 2017. Monitoring drought vulnerability using multispectral indices observed from sequential remote sensing (Case Study: Tuy Phong, Binh Thuan, Vietnam). GIScience Remote Sens. 54, 167–184. https://doi.org/10.1080/15481603.2017.1287838.

Trnka, M., Hlavinka, P., Možný, M., Semerádová, D., Štěpánek, P., Balek, J., Bartošová, L., Zahradníček, P., Bláhová, M., Skalák, P., Farda, A., Hayes, M., Svoboda, M., Wagner, W., Eitzinger, J., Fischer, M., Žalud, Z., 2020. Czech Drought Monitor System for monitoring and forecasting agricultural drought and drought impacts. Intl J. Climatology 40, 5941–5958. https://doi.org/10.1002/joc.6557.

Urban, M., Berger, C., Mudau, T.E., Heckel, K., Truckenbrodt, J., Onyango Odipo, V., Smit, I.P.J., Schmullius, C., 2018. Surface moisture and vegetation cover analysis for drought monitoring in the Southern Kruger National Park using sentinel-1, sentinel-2, and landsat-8. Remote Sens. 10, 1482. https://doi.org/10.3390/rs10091482.

Vicente-Serrano, S.M., Beguería, S., López-Moreno, J.I., 2010. A multiscalar drought index sensitive to global warming: the standardized precipitation evapotranspiration index. J. Clim. 23, 1696–1718. https://doi.org/10.1175/2009JCLI2909.1.

Wable, P.S., Jha, M.K., Shekhar, A., 2019. Comparison of drought indices in a semi-arid river basin of India. Water Resour. Manag. 33, 75–102. https://doi.org/10.1007/s11269-018-2089-z.

West, H., Quinn, N., Horswell, M., 2019. Remote sensing for drought monitoring & impact assessment: progress, past challenges and future opportunities. Rem. Sens. Environ. 232, 111291. https://doi.org/10.1016/j.rse.2019.111291.

Winkler, K., Gessner, U., Hochschild, V., 2017. Identifying droughts affecting agriculture in Africa based on remote sensing time series between 2000–2016: rainfall anomalies and vegetation condition in the context of ENSO. Remote Sens. 9, 831. https://doi.org/10.3390/rs9080831.

Wu, J., 2013. Establishing and assessing the Integrated Surface Drought Index (ISDI) for agricultural drought monitoring in mid-eastern China. Int. J. Appl. Earth Obs. Geoinf. 126, 225–244. https://doi.org/10.1016/j.isprsjprs.2017.01.019.

Yao, N., Zhao, H., Li, Y., Biswas, A., Feng, H., Liu, F., Pulatov, B., 2020. National-Scale Variation and Propagation Characteristics of Meteorological, Agricultural, and Hydrological Droughts in China.

Zekri, S. (Ed.), 2020. Water Policies in MENA Countries, Global Issues in Water Policy. Springer International Publishing, Cham. https://doi.org/10.1007/978-3-030-29274-4.

Zhang, A., Jia, G., 2013. Monitoring meteorological drought in semiarid regions using multi-sensor microwave remote sensing data. Rem. Sens. Environ. 134, 12–23. https://doi.org/10.1016/j.rse.2013.02.023.

Zhang, N., Hong, Y., Qin, Q., Liu, L., 2013. VSDI: a visible and shortwave infrared drought index for monitoring soil and vegetation moisture based on optical remote sensing. Int. J. Rem. Sens. 34, 4585–4609. https://doi.org/10.1080/01431161.2013.779046.

Zhang, X., Chen, N., Li, J., Chen, Z., Niyogi, D., 2017. Multi-sensor integrated framework and index for agricultural drought monitoring. Rem. Sens. Environ. 188, 141–163. https://doi.org/10.1016/j.rse.2016.10.045.

Zhou, L., Wu, J., Zhang, Jianhui, Leng, S., Liu, M., Zhang, Jie, Zhao, L., Zhang, F., Shi, Y., 2013. The Integrated Surface Drought Index (ISDI) as an indicator for agricultural drought monitoring: theory, validation, and application in mid-Eastern China. In: Sel. Top. Appl. Earth Observations Remote Sensing, vol. 6. IEEE, pp. 1254–1262. https://doi.org/10.1109/JSTARS.2013.2248077.